Colloid Polym Sci 280:99–106 (2002)

ORIGINAL CONTRIBUTION

T. Sakai
K. Kamogawa
K. O. Kwon
H. Sakai
M. Abe

Pyrene fluorescence measurements of metastable oil droplets in surfactant-free oil-in-water emulsions

Received: 20 June 2001
Accepted: 19 April 2001

T. Sakai · H. Sakai · M. Abe (✉)
Faculty of Science and Technology
Tokyo University of Science
2641 Yamazaki, Noda
Chiba 278-8510, Japan
e-mail: abemasa@ci.noda.sut.ac.jp
Tel.: +81-471-248650
Fax: +81-471-248650

K. Kamogawa
Ele. & Sec Ed. Bureau, The Ministry of
Education, Sports, Culture and Science
Kasumigaseki, Chiyoda
Tokyo 100-0013, Japan

K. Kamogawa · H. Sakai · M. Abe
Institute of Colloid and Interface Science
Tokyo University of Science
1-3 Kagurazaka, Shinjuku
Tokyo 162-8601, Japan

K.O. Kwon
Korea Fire Equipment Inspection
Corporation, 29-16, Shinheung-dong
3ga, Chung-ku, Inchon City
Seoul, Korea

Abstract The fluorescence behavior of pyrene in oil droplets of a surfactant-free oil-in-water emulsion was studied for benzene, fluorobenzene, *n*-hexane and cyclohexane droplets in water. The excimer–monomer fluorescence ratio immediately after sonication, $I_E/I_M(0)$, of the benzene/water emulsion was 8–10 times larger than for the benzene solution. The ratio $I_E/I_M(t)$ increased in the first 10–20 min before it decreased to zero. Similar behavior was observed for the fluorobenzene/water emulsion, while $I_E/I_M(0)$ for emulsions with *n*-hexane and cyclohexane was smaller than for benzene and fluorobenzene/water emulsions. $I_E/I_M(t)$ hardly changed with time for the *n*-hexane and cyclohexane/water emulsions. This different behavior was attributed to the increased solubility of nanometer-size droplets with benzene and fluorobenzene.

Keywords Molecular diffusion · Ostwald ripening · Surfactant-free oil-in-water emulsion · Pyrene fluorescence · I_E/I_M and I_1/I_3 ratios

Introduction

We found that surfactant-free oil-in-water emulsions (SFEs) could be prepared using an ultrasonicator [1–3]. Furthermore, the size of the oil droplets monitored by dynamic light scattering (DLS) increased discontinuously with time, and discrete droplet size distributions were observed. We named these discrete distributions with diameters at about 100 nm, 100–1,000 nm and about 1,000 nm, S, M and L class, respectively. For benzene and fluorobenzene/water emulsions three distributions appeared at 20–100 nm (S), 200–1,000 nm (M) and 2,000–4,000 nm (L), while for *n*-hexane and cyclohexane SFEs two size distributions, 100–1,000 nm (M) and 2,000–4,000 nm (L), were observed [1]. Two types of growth mechanisms have been proposed for emulsions: flocculation/coalescence and Ostwald ripening [4–11], i.e. direct fusion of two or more droplets to form a larger one and molecular diffusion/deposition from small droplets to large ones, respectively. Both schemes are expected to play a dominant role in the growth process of oil droplets, especially in surfactant-free conditions.

In the monomer spectrum of pyrene, I_1/I_3 [12–18] varies with the microscopic polarity, from 0.5 to 0.8 in organic media to 1.55 in aqueous environments [12–23]. The ratio of the excimer fluorescence intensity to the monomer intensity, I_E/I_M, represents the probability of excimer formation for pyrene molecules, in relation to the local concentration in the environment [12, 18, 20–23]. Thus, these ratios give a good insight into the hydrophobicity of oil droplets in terms of the molecular motion of pyrene. They revealed the influence of the temperature and the type and concentration of stabilizers on the microscopic behavior of molecular assemblies [24–26]. Furthermore, rapid micelle fusion and fragmentation was examined in a time-scan experiment by monitoring the change in I_M or I_E under stopped-flow conditions [27]. The dissolution process of glassy polymers was monitored by the fast transient fluorescence technique [28].

In this work, the fluorescence behavior of pyrene in oil droplets of SFEs was studied for benzene, fluorobenzene, *n*-hexane and cyclohexane droplets dispersed in water by ultrasound. We examined the influence of destabilizing processes: flocculation/coagulation, coalescence, creaming and Ostwald ripening [4–11].

Materials and methods

Benzene, *n*-hexane, cyclohexane, and fluorobenzene (Tokyo Kasei Co.) were general reagent grade and were used as received. Distilled and deionized water of injection grade (Ohtsuka Pharmacy Co.) was used without further purification. Pyrene of general reagent grade purchased from Wako was recrystallized several times from ethanol and was purified chromatographically through silica. The purity was checked and confirmed with high-sensitivity scanning calorimetry. Oil solutions of pyrene were mixed with water in a flask and kept at 25 °C. The mixture was then sonicated for 2 min in an ultrasonic cleaning bath (Bransonic 220, 125 W, SmithKline). Immediately after the treatment, the sample was transferred to a cuvette for fluorescence measurement. Deoxygenation was not applied to these solutions.

Fluorescence spectra were recorded with a fluorescence spectrometer (RF-5000, Shimazu Co.) using excitations at 335 nm. Excitation spectra were recorded at 500 nm (excimer emission). Either emission or excitation spectra were repeatedly scanned over the full range. The cell was kept at 25 °C by circulating temperature-controlled water and was sealed during the measurements to avoid vaporization. Since the emulsions were significantly turbid, we paid attention to the influence of the scattered light. The fluorescence peaks of the pyrene monomer and excimer are at around 380 and 480 nm, respectively. The transmittances at 380 and 480 nm of benzene SFE are almost identical, indicating that influence of turbidity on the fluorescence intensity could be neglected.

Results and discussion

Dependence of oil concentration on the location of pyrene molecules

$I_1/I_3(0)$ and $I_E/I_M(0)$ values of SFEs immediately after preparation ($t = 0$) at various oil concentrations are shown in Fig. 1. At low oil concentration, $I_1/I_3(0)$~1.6, indicating that pyrene monomers exist in the aqueous environment. $I_1/I_3(0)$ decreases above a certain concen-

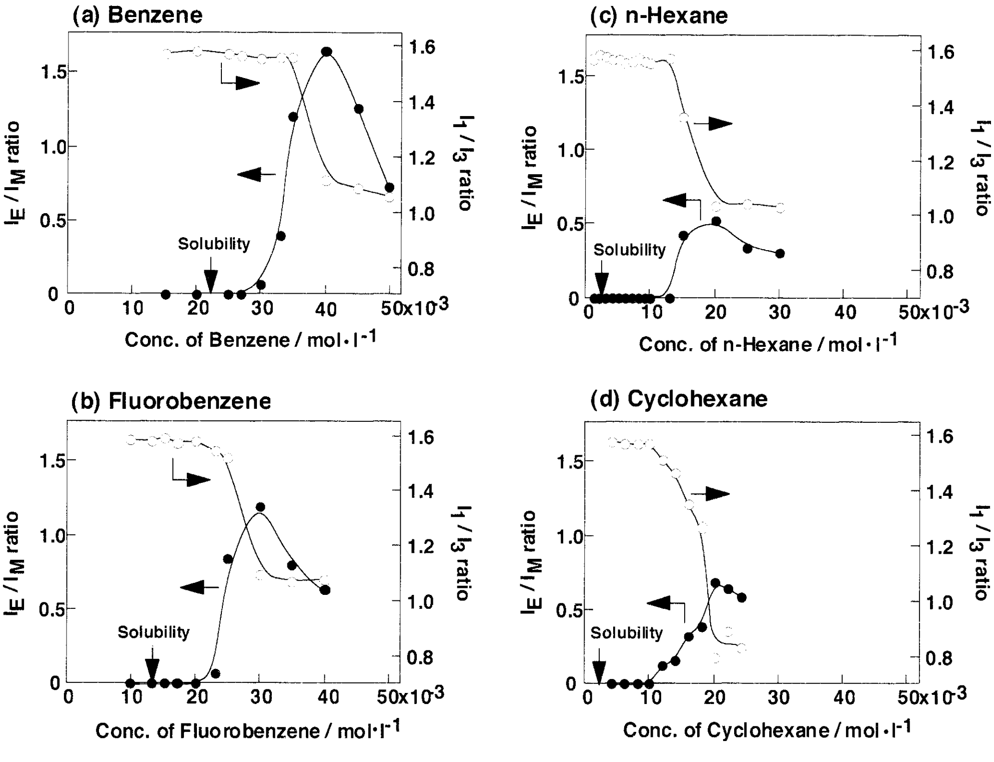

Fig. 1a–d $I_E/I_M(0)$ (*filled circles*) and $I_1/I_3(0)$ (*open circles*) for surfactant-free oil-in-water emulsions (*SFEs*) at various oil concentrations. Pyrene/oil concentration: 1.5 mmoll^{-1}

tration to around 1.1, indicating that pyrene monomers are now orientated in the oil environment. On the other hand, $I_E/I_M(0)$ is negligibly small at low oil concentrations. This also indicates that the pyrene molecules are distributed in water as monomers at low oil concentration. For benzene SFE, the $I_E/I_M(0)$ ratio rises at around 3.0×10^{-2} moll^{-1} significantly above the solubility of benzene in water at 2.3×10^{-2} moll^{-1}, and then shows a maximum at 4.0×10^{-2} moll^{-1} before decreasing at higher concentrations. A sudden rise in $I_E/I_M(0)$ is also observed for fluorobenzene SFE above about 2.0×10^{-2} moll^{-1}, which is higher than the solubility at around 1.0×10^{-2} moll^{-1}. Although a similar sudden rise is seen for *n*-hexane and cyclohexane SFEs, the maximum of I_E/I_M only reaches 0.5–0.6. The sudden rise begins at a much higher concentration (around 1.0×10^{-2} moll^{-1}) than the solubility (around 1×10^{-3} moll^{-1}). The rise and maximum reveal that pyrene excimers are formed and are only concentrated in the oil droplets. In addition, the decay above this concentration indicates that the interior environment of the oil droplet becomes similar to bulky oil, because the droplet size increases with increasing oil concentration [1].

The fluorescence excitation spectra at 500 nm at various benzene concentrations are shown in Fig. 2 for benzene SFE. The spectrum of pyrene in water has a large peak at 335 nm (Fig. 2 trace a), while that in benzene shows a broad peak above 350 nm (Fig. 2 trace e). Fig. 2 traces b, c and d are spectra at various concentrations of benzene dispersed in water: 2.0, 3.0 and 3.5×10^{-2} moll^{-1}. In Fig. 2 trace b, several peaks around 335 nm can be assigned to the band for hydrated pyrene and the peaks above 350 nm can be assigned to pyrene in oil. With increasing benzene concentration (Fig. 2 traces c, d), the peak at 335 nm was enhanced. This indicates that pyrene molecules orient to the interface between benzene droplets and water. Furthermore, the peak at 335 nm for the hydrated state shifted to 340 nm at 3.0–3.5×10^{-2} moll^{-1} benzene. These results and the behavior of $I_E/I_M(0)$ (Fig. 1) indicate that the excimer-forming sites lie in or near the surface of the droplets. This idea that pyrene molecules orient to the interface between the oil droplets and water seems to be strange according to the hydrophobic/hydrophilic balance of pyrene. However, when a mixture of benzene and small amounts of *n*-hexadecane is emulsified in water, *n*-hexadecane adsorbs to the interface between the benzene droplets and water [2, 7]. We consider that pyrene molecules behave in a similar way as *n*-hexadecane.

The excitation spectra for *n*-hexane SFE are shown in Fig. 3. Peaks appeared at almost the same wavelengths as for benzene SFE. Several peaks around 335 nm again can be assigned to the band for hydrated pyrene and the peaks above 350 nm can be assigned to pyrene in oil. The slight peak shift to 340 nm in benzene SFE is not observed for *n*-hexane SFE even at high *n*-hexane concentrations. This indicates that the excimer-forming sites are limited to the droplet surface even at higher *n*-hexane concentrations.

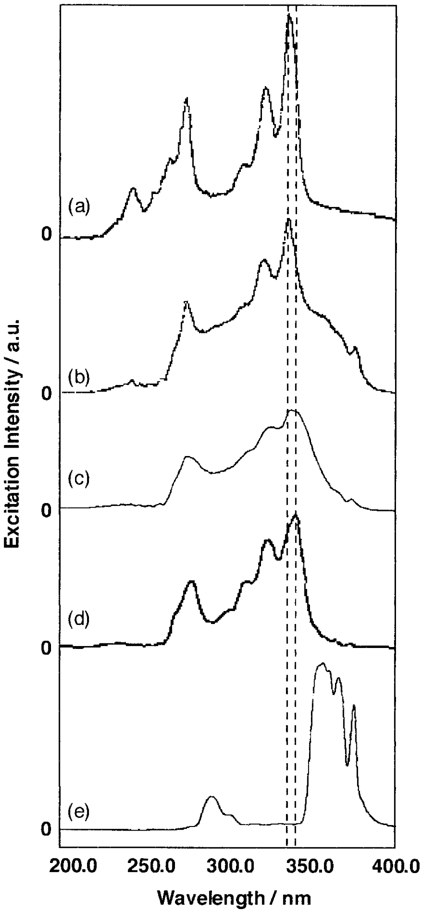

Fig. 2 Excitation spectra of benzene SFE in water at various benzene concentrations: $\lambda_{em} = 500$ nm. (*a*) 0 moll^{-1} (pyrene at 20μmoll^{-1} in water), (*b*) 20 mmoll^{-1}, (*c*) 30 mmoll^{-1} and (*d*) 35 mmoll^{-1}. (*e*) Benzene stock solution with 1.5 mmoll^{-1} pyrene

Enhanced excimer formation in oil droplets

The emission spectra of pyrene in benzene and benzene SFE immediately after sonication at the oil concentration corresponding to the maximum of $I_E/I_M(0)$ (Fig. 1) are shown in Fig. 4. The emission intensity of excimers for the emulsion is significantly larger than for benzene.

$I_E/I_M(0)$ is shown as a function of pyrene concentration in various solvents in Fig. 5. Excimers were formed at pyrene concentrations above about 0.5 mM. In all cases, $I_E/I_M(0)$ of the emulsions increased linearly and showed larger values than in the pure solution. The enhancement was about 10 times for benzene, about 8 times for fluorobenzene and only

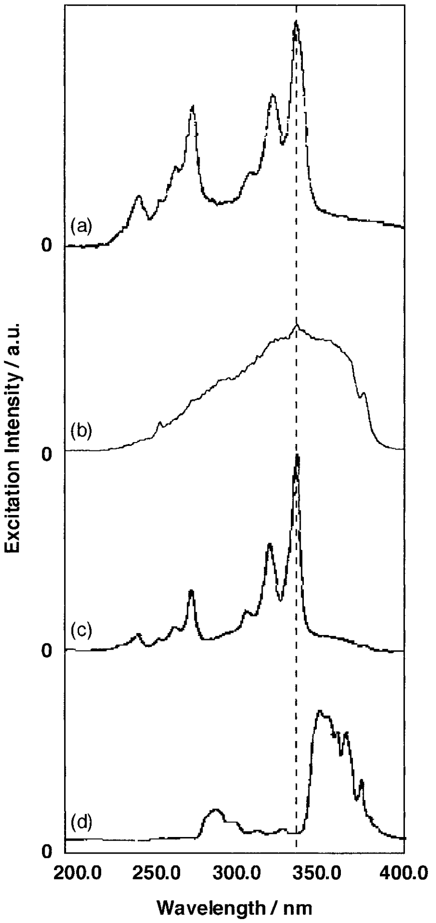

Fig. 3 Excitation spectra of *n*-hexane SFE in water at various *n*-hexane concentrations: $\lambda_{em} = 500$ nm. (*a*) 0 moll^{-1} (pyrene at 20μmoll^{-1} in water), (*b*) 5 mmoll^{-1} and (*c*) 15 mmoll^{-1}. (*d*) *n*-Hexane stock solution with 1.5 mmoll^{-1} pyrene

slightly larger for *n*-hexane and cyclohexane than for stock solutions. This result suggests that benzene and fluorobenzene droplets have a peculiar region where pyrene molecules are condensed.

Time dependence of the intensities

For benzene SFE, $I_E/I_M(t)$ increased in the initial 15 min to a maximum and then decreased to nearly zero. This rise corresponds to the transient appearance of S-class droplets in the first 20 min [1]. For fluorobenzene SFE, the appearance of the maximum was delayed, depending on the pyrene concentration, in contrast to the case of benzene SFE, where the maximum occurred at the same time.

The maxima of $I_E/I_M(t)$ (Fig. 6) and the high value of $I_E/I_M(0)$ immediately after sonication (Fig. 5) for benzene and fluorobenzene SFEs can be explained in terms of Ostwald ripening [4–10]. The diffusion from oil droplets leads to shrinkage or disappearance of droplets. This indicates that pyrene initially dissolved in small droplets will be concentrated inside the droplets with time and then released to the bulk water. Indeed, the intensity of the monomer emission became higher than that of the excimer about 10 min after preparation (Fig. 7). Benzene has a relatively high solubility in water compared to aliphatic oils. The larger droplets can grow at the expense of the smaller ones. The magnitude of this effect depends on the solubility of the oil phase and is therefore larger for polar oils and shorter-chain alkanes. Furthermore, nanometer-size droplets have a higher vapor pressure to increase the solubility of the oil in the surrounding medium based on the Laplace pressure [29, 30]. The droplet size observed by DLS in benzene and fluorobenzene SFEs was around 30 nm in diameter [1]. According to the Ostwald–Friedrich theory [18, 31, 32], oil droplets of such sizes can be dissolved by molecular diffusion in water. An oil droplet with radius *r* will be at a dynamic equilibrium with the dissolved oil molecules at a concentration of S_r as long as the oil has a solubility of S_e at the steady state of the two-phase equilibrium ($r = \infty$):

$$RT\ln(S_r/S_e) = 2\gamma V_m/r \ , \qquad (1)$$

where γ and V_m denote the interfacial tension between oil and water and the molar volume of the oil. $I_E/I_M(0)$ rises in benzene at 30 mmoll^{-1}, i.e. 30% higher than the solubility limit. This indicates $S_r/S_e \approx 1.3$. With $\gamma \approx 35$ mN and $V_m = 89.4$ cm^{3}mol^{-1} at 298 K, $r \approx 10$ nm was obtained. The value is similar to the observed diameter of around 30 nm of S-class droplets of benzene [1]. The increase in $I_E/I_M(t)$ at about 10 min is consistent with the appearance of S-class droplets observed by DLS [1]. This coincidence supports the idea that the pyrene molecules dissolved in S-class droplets are concentrated in the droplets of reduced sizes by dissolution of the droplets.

Molecular diffusion may also be responsible for another property of the droplets. Benzene SFE prepared with ultrasound showed a continuous change in refractive index and density below a benzene concentration of 30 mmoll^{-1}, while for benzene/water mixtures prepared with gentle stirring these quantities changed at 23 mmoll^{-1} [1]. This difference in the preparation method probably caused different dissolution behavior of benzene molecules, which may effect the droplet radius. Thus, gentle stirring provided visible droplets and S_r is nearly equal to S_e in Eq. (1).

No maximum was observed for *n*-hexane and cyclohexane SFEs prior to the monotonous decay of $I_E/I_M(t)$. Molecular diffusion does not play a role, because *n*-hexane and cyclohexane have a distinctly lower solubility in water than benzene and fluorbenzene, and S-class droplets are not created. The droplets of *n*-hexane and cyclohexane in the SFEs thus keep their individual characteristics even when the M droplet size changes into L.

$I_1/I_3(t)$ as a function of time is also shown in Fig. 8 for various pyrene concentrations for oil concentrations at the maximum value of $I_E/I_M(0)$ (Fig. 1). $I_1/I_3(t)$ decreased in the first 10–20 min before it increased. This

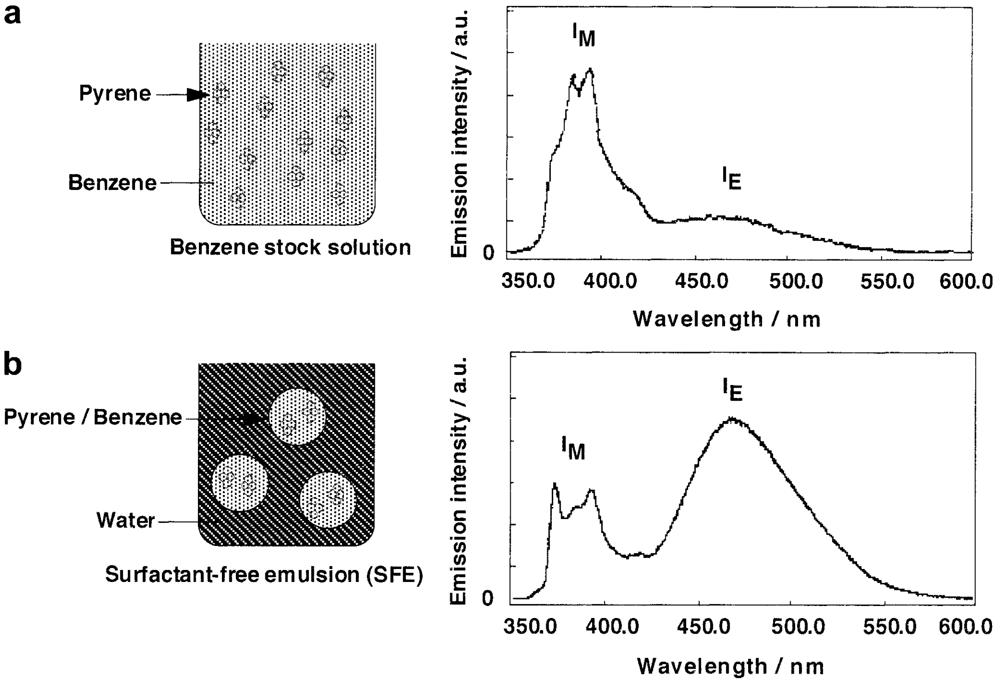

Fig. 4 Emission spectra of pyrene in **a** benzene stock solution and **b** benzene SFE immediately after preparation (40 mmoll^{-1} benzene in water): $\lambda_{exc} = 335$ nm. Pyrene concentration in benzene:1.5 mmoll^{-1}

(a) Benzene

(c) n-Hexane

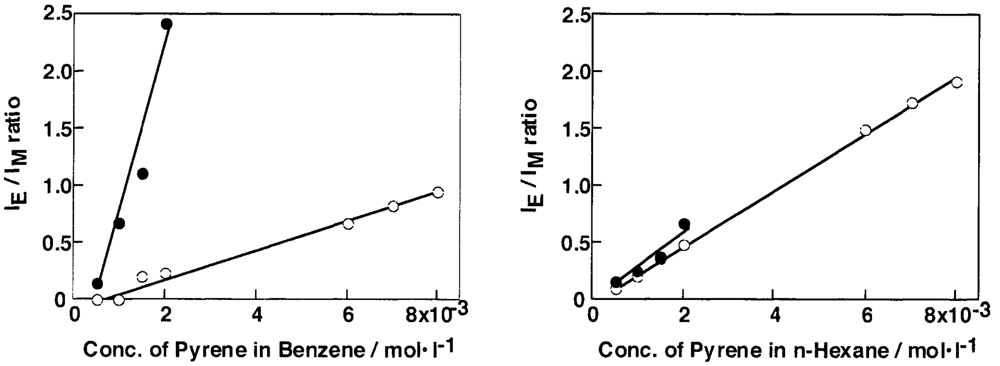

(b) Fluorobenzene

(d) Cyclohexane

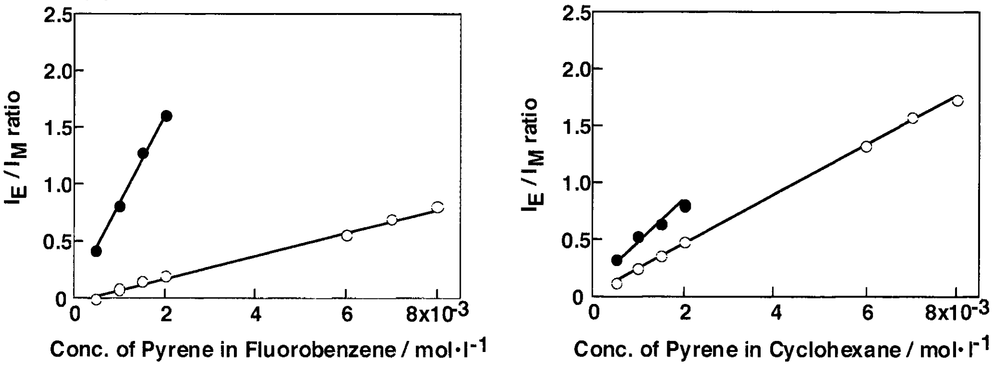

Fig. 5 $I_E/I_M(0)$ for various solvents (*open circles*) and their emulsions (*filled circles*) as a function of pyrene concentration. **a** Benzene 40 mmoll^{-1} water, **b** fluorobenzene 30 mmoll^{-1} water, **c** *n*-hexane 20 mmoll^{-1} water, **d** cyclohexane 20 mmoll^{-1} water

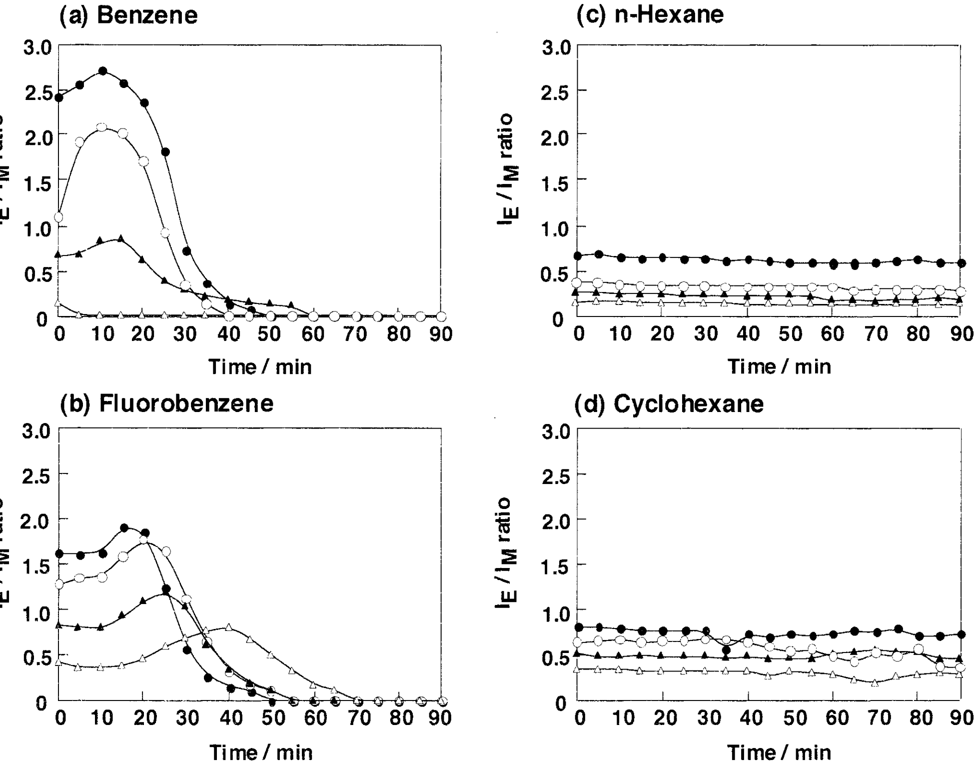

Fig. 6a–d $I_E/I_M(t)$ for SFEs as a function of time at several pyrene concentrations. The oil concentration corresponds to the maximum of $I_E/I_M(0)$ (Fig. 1). Pyrene concentration: 2.0 mM (*filled circles*), 1.5 mM (*open circles*), 1.0 mM (*filled triangles*), 0.5 mM (*open triangles*). Oil concentration: **a** benzene 40 mmoll^{-1} water, **b** fluorobenzene 30 mmoll^{-1} water, **c** *n*-hexane 20 mmoll^{-1}water, **d** cyclohexane 20 mmoll^{-1} water

tend was observed for all oils except *n*-hexane, for which I_1/I_3 remained at 1.0–1.2. This value indicates a significant hydrophobic environment, similar to the case of sodium dodecyl sulfate micelles, where I_1/I_3 is 1.0–1.1 [33, 34]. The initial decrease of $I_1/I_3(t)$ shows that, with increasing time, pyrene molecules are gradually concentrated in the oil droplets. $I_1/I_3(t)$ finally reaches 1.55 for benzene and fluorobenzene SFEs, showing an aqueous environment. This change in $I_1/I_3(t)$ was caused by the diffusion of oil molecules into bulk water and Ostwald ripening; only the monomer emission of pyrene in water is finally detected (Fig. 7). For *n*-hexane and cyclohexane SFEs, $I_1/I_3(t)$ finally increases to around 1.4, indicating that the contribution of diffusion is smaller.

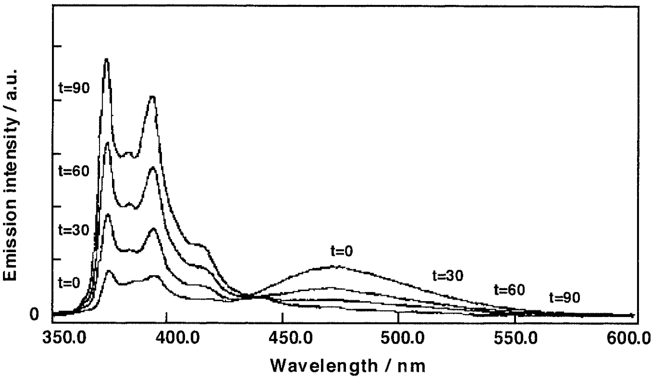

Fig. 7 Emission spectra for benzene SFE at different times after preparation: $\lambda_{exc} = 335$ nm

In this study, we showed that the temporal changes of $I_E/I_M(t)$ and $I_1/I_3(t)$ for SFE are caused by molecular dissolution of S-class small droplets. On the other hand, we observed the coalescence of the M-class droplets in benzene, *n*-hexane and cyclohexane SFEs by freeze–fracture electron microscopy [35]. Thus, the changes of the oil droplets vary depending on droplet size; molecular diffusion and coalescence occur, respectively, when droplets are of nanometer size (S class) and submicron size (M class). If the growth process of benzene and fluorobenzene droplets is caused only by coalescence, $I_E/I_M(t)$ should be constant or decrease monotonously with time, and a maximum should not appear. For *n*-hexane and cyclohexane SFEs, $I_E/I_M(t)$ remains almost constant, though the size observed by DLS changed from around 300 nm to around 3,000 nm in diameter with time. This suggests that the growing process of *n*-hexane and cyclohexane is governed by coalescence.

Conclusions

Fluorescence measurements with pyrene provide valuable information on molecular dissolution of oil droplets dispersed in water. A significant difference in the growing processes between benzene and fluoro-

Fig. 8a–d $I_1/I_3(t)$ for SFEs as a function of time at several pyrene concentrations. The oil concentration corresponds to the maximum of the $I_E/I_M(0)$ (Fig. 1). *Symbols* same as in Fig. 6

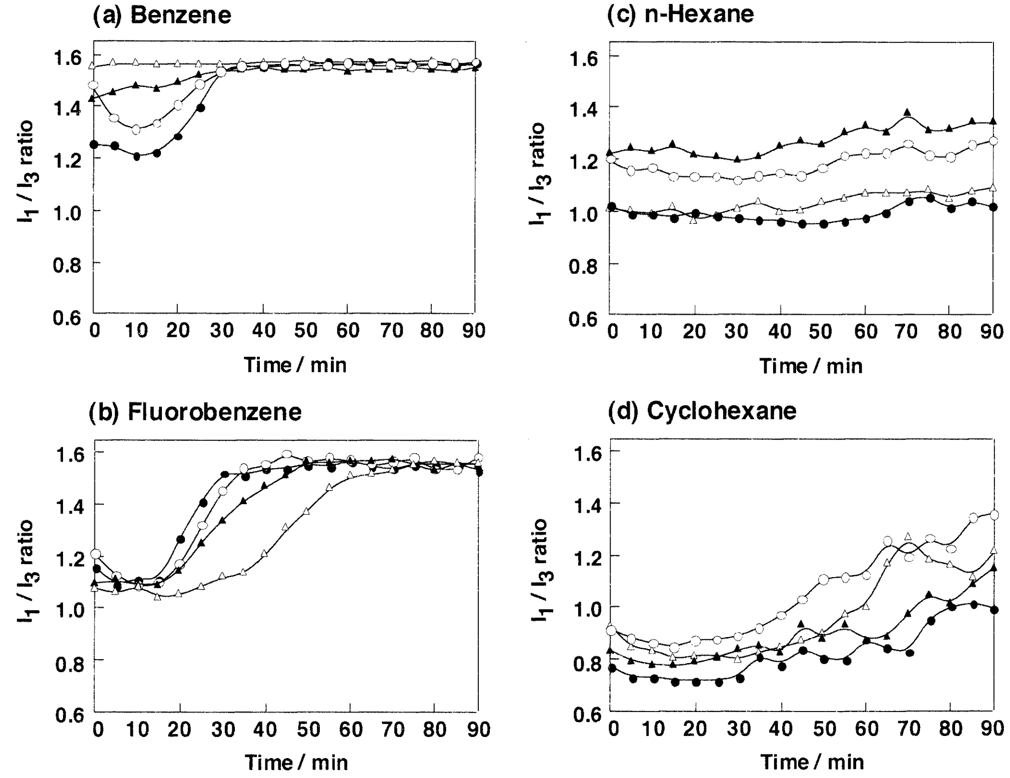

benzene and *n*-hexane and cyclohexane was observed. The fluorescence of pyrene in benzene and fluorobenzene shows time-dependent spectral changes. Benzene and fluorobenzene droplets with nanometer size dissolve in water and pyrene molecules in the droplets are released into the bulk water, causing a change in the fluorsecence spectra. The fluorescence spectra of *n*-hexane and cyclohexane droplets of submicron size do not change, because the solubility of the hydrocarbon is smaller.

Acknowledgement The authors are grateful to the Cosmetology Research Foundation for financial support in the realization of this work.

References

1. Kamogawa K, Sakai T, Momozawa N, Shimazaki M, Enomura M, Sakai H, Abe M (1998) J Jpn Oil Chem Soc 47:159
2. Kamogawa K, Matsumoto M, Kobayashi T, Sakai T, Sakai H, Abe M (1999) Langmuir 15:1913
3. Kamogawa K, Akatsuka H, Matsumoto M, Yokoyama S, Sakai T, Sakai H, Abe M (2001) Colloids Surf A 180:41
4. Evans DF, Wennersrrom H (1999) The colloidal domain, 2nd edn. Wiley-VCH, New York
5. McClements DJ (1998) Food emulsions: practice and techniques. CRC, Boca Raton
6. Hunter RJ (1986) Foundations of colloid Science, vol 1. Oxford University Press, Oxford
7. Davis SS, Smith A (1976) In: Smith AL (ed) Theory and practice of emulsion technology. Academic, London, pp 325–349
8. Binks BP (1998) In Binks BP (ed) Modern aspects of emulsion science. Royal Society of Chemistry, Cambridge, pp 1–55
9. Taylor P (1995) Colloids Surf A 99:175
10. Taylor P (1998) Adv Colloid Interface Sci 75:107
11. Higuchi WI, Misra J (1962) J Pharm Sci 51:459
12. Kano K (1988) Rev Top Surf Sci Technol Avant-garde 26:243
13. Kalyanasundaram K, Thomas JK (1977) J Am Chem Soc 99:2039
14. Nakajima A (1971) Bull Chem Soc Jpn 44:3272
15. (a) Nakajima A (1976) J Mol Spectrosc 61:467; (b) Nakajima A (1977) J Lumin 15:277
16. Kano K, Yanagimoto M, Hashimoto S (1986) Bull Chem Soc Jpn 59:3451
17. Dong DC, Winnik M (1982) Photochem Photobiol 35:17
18. Thomas JK (1980) Chem Rev 80:283
19. Turro NJ, Yekta A (1978) J Am Chem Soc 100:5951
20. Galla HJ, Sachman E (1973) Biochim Biophys Acta 339:103
21. Dembo M, Glushko V, Aberlin ME, Sonenberg M (1979) Biochim Biophys Acta 522:201
22. Soutar AK, Powrall HJ, Hu AS, Smith LC (1974) Biochemistry 13:2828
23. Pownall HJ, Smith LC (1973) J Am Chem Soc 95:3136

24. Castanheira EMS, Martinho JMG, Duracher D, Charreyre MT, Elaissari A, Pichot C (1999) Langmuir 15:6712
25. Ewa S-P, Marian W, Andrzej P, Shulamith S (1999) Macromolecules 32:7454
26. Kim J-H, Domach MM, Tilton RD (1999) J Phys Chem B 103:10582
27. Rharbi Y, Winnil MA, Hahn KG Jr (1999) Langmuir 15:4697
28. Ugur S, Pekcan O (2000) Polymer 41:1571
29. Defay R, Prigogine I, Bellemans A, Everett DH (1966) Surface tension and adsorption. Wiley, New York
30. Menger FM (1979) J Phys Chem 83:893
31. Thomson W (1871) Proc R Soc Edinburgh 7:63
32. Buscall R, Davis SS, Potts DC (1979) Colloid Polym Sci 257:636
33. Hunter RJ (1989) Foundations of colloid science. Clarendon, Oxford, p 601
34. Ito A, Kamogawa K, Sakai H, Kondou Y, Yoshino N, Abe M (1996) J Jpn Oil Chem Soc 45:479
35. Sakai T, Kamogawa K, Harusawa F, Momozawa N, Sakai H, Abe M (2001) Langmuir 17:255